

Modulation of oscillatory brain activity and evoked potentials in a repetition priming task in the human EEG

Thomas Gruber,¹ Peter Malinowski² and Matthias M. Müller¹

¹Institut für Allgemeine Psychologie, Universität Leipzig, Leipzig, Germany

²School of Psychology, Liverpool John Moores University, Liverpool, UK

Keywords: induced gamma band response, phase-locking, repetition priming, repetition suppression, synchrony, vision

Abstract

Cortical object representations seem to require the formation of neural cell assemblies. The physiological correlate of cell assembly activity may be seen in synchronized neural activity in the gamma band range. The improvement in perceiving and identifying an object by experience is commonly referred to as repetition priming. One possible neural mechanism for repetition priming is 'repetition suppression' within a cell assembly coding the stimulus. The present electroencephalogram study was designed to investigate oscillatory brain activity when line drawings of concrete objects were repeated either immediately after a first presentation or after intervening a number of different stimuli. Results showed a broad posterior distribution of induced gamma band responses (GBRs) after the initial picture presentation. Repeated presentations of the same picture led to a significant decrease of induced gamma power. Furthermore, repeated presentations of the same object resulted in a decrease in phase synchrony between distant electrode sites. No significant repetition effects were found in the alpha or beta frequency range. The event-related potential (ERP), which was also modulated by priming, showed a different scalp distribution compared with induced GBRs. In addition, ERP repetition effects decayed at larger intervals between initial and repeated presentations, whereas induced GBRs were not modulated as a function of stimulus lag. We concluded that the decrease in amplitude of induced GBRs and the reduction of gamma phase synchrony between pairs of electrodes after repeated picture presentations might be linked to a 'sharpening' mechanism within a cell assembly representing an object.

Introduction

Facilitation in perception to repeated stimuli is commonly referred to as repetition priming (Tulving & Schacter, 1990). A neural correlate associated with repeated stimulus processing is a reduced firing rate of neurons (Brown & Aggleton, 2001), an effect termed 'repetition suppression' (Schacter & Buckner, 1998). Recently, Wiggs & Martin (1998), elaborating on ideas of Desimone (1996), suggested that repetition suppression is a by-product of a 'sharpening' of cortical object representations. In this view, experience leads to representations, which are limited to the essential object features. This sparser representation allows more efficient stimulus processing, which can result in behavioural priming effects, such as shorter reaction times (RTs).

In general, cortical object representations are considered to be activated by synchronization of neuronal activity within cell assemblies, which represent various stimulus features and can be distributed across different brain areas (Milner, 1974; Malsburg & Schneider, 1986; Singer & Gray, 1995). Induced gamma band responses (GBRs) are discussed as a signature of such a cell assembly (Tallon-Baudry & Bertrand, 1999; Keil *et al.*, 2001). Empirical evidence for that notion was provided by studies that showed that learned representations of a stimulus induced GBRs in the human electroencephalogram (EEG, Pulvermüller, 1996; Gruber *et al.*, 2001, 2002). A further measure, which might provide information regarding the establishment of a cell assembly, is phase synchrony between electrode sites. It was shown

that phase-locking between electrodes is only present when subjects perceived an object (Rodriguez *et al.*, 1999) or have learned an association between stimuli (Miltner *et al.*, 1999).

Consequently, in a previous repetition priming experiment, we analysed spectral power and phase synchrony to draw a more conclusive picture of neural cell assembly activity and the effects of repetition priming upon these measures. We found a reduction of GBRs and a decrease in phase synchrony after immediate picture repetition, which we interpreted as a signature of sharpening of a network coding an object (Gruber & Müller, 2002). In this study, however, we repeated stimuli without intervening pictures. As a consequence, we were not able to exclude habituation as an alternative explanation for our results. The present experiment was designed to exclude this alternative and to extend our previous findings. Therefore, we repeated pictures not only directly after the first presentation but also after intervening a number of different stimuli.

Based on the above hypothesis, we expected that picture repetition leads to a 'sharpening' within an object representation. Notwithstanding the fact that repeated stimuli have to be coded by synchrony within cell assemblies, due to spatial summation in macroscopical EEG recordings, we hypothesized that the activation of a sparser network should result in a reduction of induced GBR power and phase synchrony.

Besides induced oscillatory activity, we analysed the event-related potential (ERP) elicited by initial and repeated stimuli. It was hypothesized that ERPs play a functionally different role opposed to induced GBRs (Tallon-Baudry & Bertrand, 1999; Gruber *et al.*, 2002). If this hypothesis is true, we must find different characteristics of repetition effects in the ERP and induced GBRs.

Correspondence: Dr T. Gruber, as above.
E-mail: gruber@rz.uni-leipzig.de

Received 21 August 2003, revised 19 November 2003, accepted 1 December 2003

Materials and methods

Subjects

Twelve healthy, right-handed university students (nine female, three male) received class credits for participation. Their age ranged from 19 to 21 years (mean 19.5 years, SD 0.67 years). All had normal or corrected-to-normal visual acuity. Informed consent was obtained from each participant. The study conformed with the Code of Ethics of the World Medical Association.

Stimuli and task

Stimuli were 260 line drawings taken from the Snodgrass & Vandervort (1980) inventory in their unfragmented version, which were presented in the centre of a 19-inch computer screen placed 1.5 m in front of the subjects with a frame rate of 70 Hz. A white fixation square of 0.3×0.3 degrees of visual angle was always present in the centre of the screen. The line drawings covering a visual angle of approximately 4.5×5.2 degrees were shown in white on a black background. Picture onset was synchronized to the vertical retrace of the monitor.

Each line drawing was presented twice. Pictures were repeated either in the directly succeeding trial after the initial presentation (LAG 0), after intervening one different picture (LAG 1), or after intervening four different pictures (LAG 4). Figure 1I depicts an excerpt of stimulus sequence. In order to acquire RT data, subjects were instructed to respond to rare targets (pictures of animals) by pressing a button as fast as possible. Identical to other stimuli, targets were repeated with LAG 0, LAG 1 or LAG 4. No other animal stimulus was presented in between two presentations with LAGs 1 or 4.

The design resulted in two experimental conditions: (i) initial picture presentations; and (ii) repeated picture presentations. Conditions were presented in randomized order and can be subdivided according to their position within the stream of pictures: initial presentation (Fig. 1A, C and E); and repeated presentations with LAG 0 (Fig. 1B), LAG 1 (Fig. 1D) or LAG 4 (Fig. 1F). The likelihood for each of the three lags for non-animal pictures was 0.27. The likelihood for each lag for target presentations was 0.07. The experiment consisted of 510 trials. Target trials were excluded from further EEG analysis (~ 100) in order to exclude possible interference with the motor response. For every initial presentation a new picture was chosen randomly from the Snodgrass picture pool.

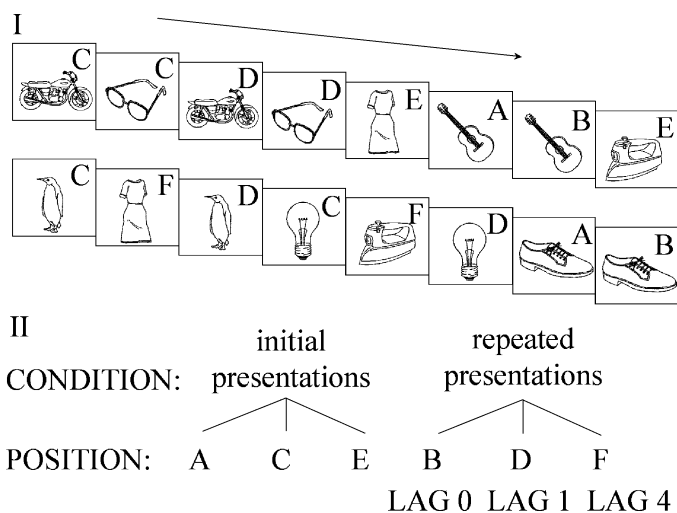


FIG. 1. (I) Excerpt of stimulus sequence. Pictures are presented for a first time (A, C and E) and Repeated for a second time with either LAG 0 (B), LAG 1 (D) or LAG 4 (F). (II) Repeated measurement ANOVA model used for statistical analysis.

Each trial consisted of a 500-ms baseline period (black screen), 700-ms picture presentation time and an inter-stimulus interval between 1100 and 1600 ms. Whenever the subject pressed the button to indicate the identification of a target, the next trial was started with an additional delay of 500 ms. Subjects were instructed to avoid eye movements and blinking while attending the pictures and to maintain their gaze to the fixation square in the middle of the screen. The experimental design was divided into three blocks of 170 trials each, in order to allow for resting intervals.

Data analysis: behavioural data

Only RTs between 200 and 1000 ms after target onset were considered to be correct responses. RTs shorter or longer than that period were seen as false alarms or missed responses.

Behavioural data were analysed by means of a repeated measurement ANOVA with the factors CONDITION (initial presentations vs. repeated presentations) \times POSITION (three). A schematic graph ANOVA model is given in Fig. 1II. The POSITION factor was introduced to test the reliability between the three first picture presentations and to examine differences between LAG 0, LAG 1 and LAG 4. Post-hoc comparisons were calculated by means of paired *t*-tests.

Electrophysiological recordings

EEG was recorded continuously with an EGI (Electrical Geodesics, Eugene, OR, USA) 128-electrode array. A schematic representation of the electrode array and corresponding extended international 10–20 electrode sites is given in Fig. 2. The vertex (recording site Cz) was chosen as reference. As suggested for the EGI high-input impedance amplifier, impedances were kept below 50 k Ω . Sampling rate was 500 Hz and all channels were pre-processed on-line by means of 0.01–200 Hz band-pass filter. In addition, vertical and horizontal eye movements were monitored with a subset of the 128 electrodes. Further data processing was performed off-line.

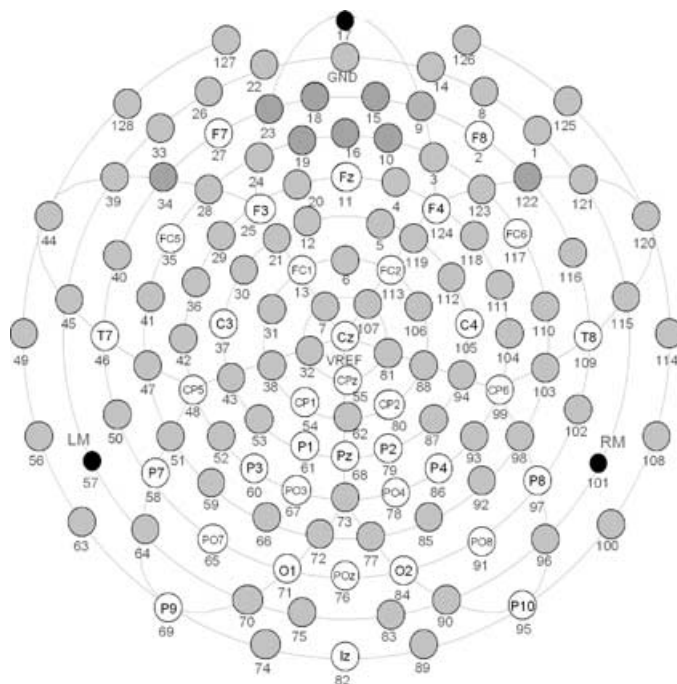


FIG. 2. Schematic representation of 128 channels montage. Extended 10–20 sites used for statistical analysis are given. Note: 10–20 sites were approximated to the closest electrode position on the net.

Data reduction and analysis

EEG was segmented to obtain epochs from 500 ms prior and 1200 ms after stimulus onset. Artefact correction was performed by means of the 'statistical correction of artefacts in dense array studies' (SCADS) procedure developed by Junghöfer *et al.* (2000). This procedure uses a combination of trial exclusion and channel approximation based on statistical parameters of the data. Firstly, global artefacts stemming from single electrodes are detected using the recording reference (Cz) and the average reference. In the next step, distinct sensors from particular trials are removed on the basis of the distribution of their amplitude, standard deviation and gradient. The information of eliminated electrodes is replaced with a statistically weighted spherical interpolation from the full channel set. The limit for the number of approximated channels was set to 20 channels. With respect to the spatial arrangement of the approximated sensors, it was ensured that rejected sensors were not located within one region of the scalp, as this would make interpolation for the area invalid. Single epochs with excessive eye movements and blinks, or artefacts on more than 20 channels were discarded. Using this method, three subjects were excluded due to excessive artefacts. For the remaining nine subjects, the average rejection rate was approximately 20% resulting in about 55 remaining trials per condition. For further analysis, the average reference was used, which – given our high spatial sampling – provides a good approximation of an inactive reference (Junghöfer *et al.*, 1999), preferable for phase-locking analysis described below.

Data analysis: induced and evoked spectral changes

A given EEG-epoch can be modelled by the sum of the evoked response plus the trial-by-trial fluctuation around the mean (Priestley, 1988). Because the present analysis focused on non phase-locked oscillatory activity, the evoked response (i.e. the ERP) was subtracted from each trial [see also: Müller *et al.* (1996), for a similar procedure]. Spectral changes in oscillatory activity during the experiment were analysed by means of a Morlet wavelet analysis of artefact-free single epochs. This method provides a good compromise between time and frequency resolution (Tallon-Baudry & Bertrand, 1999), in particular time resolution of this procedure increases with frequency, whereas frequency resolution decreases. The present procedure has been proposed by Bertrand & Pantev (1994) and is described in detail elsewhere, e.g. by Tallon-Baudry *et al.* (1997, 1998). In brief, the method provides a time-varying magnitude of the signal in each frequency band, leading to a time by frequency (TF) representation of the signal. TF energy is averaged across single trials, allowing one to analyse non phase-locked components. To that end, complex Morlet wavelets g can be generated in the time domain for different analysis frequencies f_0 according to

$$g(t, f_0) = A' e^{-\frac{t^2}{2\sigma_f^2}} e^{2i\pi f_0 t} \quad (1)$$

with A' depending on the parameter σ_f , specifying the width of the wavelet in the frequency domain, the analysis frequency f_0 and the user-selected ratio m :

$$A' = \sigma_f \sqrt{2\pi^3} \sqrt{\frac{m}{f_0 \sqrt{\pi}}} \quad (2)$$

with

$$m = f_0 / \sigma_f \quad (3)$$

and

$$\sigma_t = m / 2\pi f_0 \quad (4)$$

Thus, given a constant ratio m , the width of the wavelets in the frequency domain, σ_f , and in the time domain, σ_t , changes as a function of the analysis frequency f_0 .

In order to achieve good time and frequency resolution in the gamma frequency range, the wavelet family used is defined by a constant $m = f_0 / \sigma_f = 7$, with f_0 ranging from 2.44 to 97.65 Hz in 0.49-Hz steps. For the lower frequency range (<20 Hz), a ratio of $m = 14$ was chosen [see Tallon-Baudry *et al.* (2001) for a similar procedure]. Wavelets were normalized in order to have equal amounts of energy. For each epoch, time-varying energy in a given frequency band was calculated, this being the absolute value of the convolution of the signal with the wavelet for each epoch and each complex spectrum. An epoch from 400 to 100 ms prior to stimulus onset was used as a baseline period. The mean of this baseline was subtracted from TF matrices for each frequency and time point for each electrode, respectively.

In order to define the induced gamma frequency range and to identify the latency of the induced gamma power peak, mean spectral power averaged across all experimental conditions and across posterior electrode sites (corresponding 10–20 positions: Cp1, Cp2, P1, P3, PO3, CPz, Pz, PO4, P2, P4, P7, PO7, O1, POz, O2, PO8, P8; see Fig. 2) was represented in a TF-plot for the 20–100 Hz range. Electrode sites used for the TF-plot were selected on the basis of previous findings regarding visual information processing (Tallon-Baudry & Bertrand, 1999) and findings of our previous repetition priming study (Gruber & Müller, 2002). For further statistical analysis, a time window centred around the gamma peak and 36 electrode sites corresponding to the extended 10–20 system was used (see below). Figure 2 depicts the utilized 10–20 sites, which were approximated to the closest electrode position on the net. Due to inter-individual differences in the gamma peak frequency, for each subject the wavelet designed for the frequency of his/her maximal power in the gamma range was chosen. This peak was analysed by means of a repeated measurement ANOVA with the factors CONDITION (initial presentations vs. repeated presentations) \times POSITION (three) \times RECORDING SITE (36 electrodes). A schematic graph ANOVA model is given in Fig. III.

To analyse the time course of spectral gamma power, the mean across electrode sites showing maximum amplitudes (see below) was calculated and subjected to a repeated measurement ANOVA with the factors CONDITION (initial presentations vs. repeated presentations) \times POSITION (three) \times TIME WINDOW (before peak, peak, and after peak). The time windows before and after the peak had the same length as the gamma peak window (70 ms) and did not overlap. Furthermore, in each time window the regional mean was tested against baseline by means of one-group t -tests for initial and repeated picture presentations, respectively. Furthermore, we tested the baseline (mean power 400–100 ms prior to stimulus onset) with a similar ANOVA model to ensure that the expected reduction in gamma power is not due to differences in baseline values.

To depict the topographical distributions of the induced gamma peak, a difference topography (initial minus repeated presentations) was generated on the basis of all 128 electrode sites using an algorithm developed by Junghöfer *et al.* (1997).

To control for effects in other frequency bands, a CONDITION (initial presentations vs. repeated presentations) \times POSITION (three) \times RECORDING SITE (36 electrodes) ANOVA was calculated for the alpha band (8–12 Hz) and the beta band (15–25 Hz). Time windows for the alpha and beta frequency analysis were chosen on the basis of a TF-plot for a lower frequency range (<20 Hz) averaged across identical posterior electrode sites as for the gamma range.

To verify that our findings were due to induced and not to evoked gamma activity, the same analysis used for induced gamma responses

was applied to the spectra of the averaged and unfiltered evoked response. Because visual inspection of TF-plots for the evoked gamma response revealed no clear peak in the frequency domain, the identical frequencies, which have been identified for the induced response, were used for statistical analysis.

Data analysis: phase synchrony

Phase synchrony analysis was performed, elaborating on procedures suggested by Rodriguez *et al.* (1999) and Tallon-Baudry *et al.* (2001), which provides a method of measuring synchronous oscillatory activity independent of the signal's amplitude. For each subject, phase synchrony was computed for a narrow band-filtered signal ($f_0 \pm 3$ Hz; see also Rodriguez *et al.*, 1999 for a distinct frequency f_0 of his/her maximal gamma activity). Phase was measured by convoluting the signal with a complex Morlet wavelet designed for f_0 (see above). A complex phase value ρ was then computed at frequency f_0 , for each electrode, each time bin and each trial by dividing the result of the convolution by the magnitude of this result.

According to Tallon-Baudry and co-workers, subsequently a phase-locking value was computed for each time-point t and trial j as:

$$\rho_{k,l} = \left| \frac{1}{N} \sum e^{i(\rho_{j,k}(t,f_0) - \rho_{j,l}(t,f_0))} \right| \quad (5)$$

where N is the number of trials, k and l are the index for the pair of electrodes to be compared. For the sake of data reduction, phase-locking values were computed only for a subset of the 128-channel set, corresponding to 36 electrode sites of the extended 10–20 system (see Fig. 2). $\rho_{k,l}$ results in a real value between one (constant phase differences) and zero (random phase differences). These values were normalized by subtracting the mean value of the baseline period (black screen; 400–100 ms before stimulus onset) and dividing by the standard deviation of this time window (see Rodriguez *et al.*, 1999 for a similar procedure). To provide a topographical representation of phase-locking values over individual pairs of electrodes in a distinct time window, a statistical randomization technique was used. Time windows were chosen according to the peak of the induced GBRs, two non-overlapping time windows of 70 ms (time domain) before the gamma peak, and one time window after the gamma peak. Averaged phase synchrony for these time windows ($W_{k,l}$) between electrodes k and l were calculated. For each of these averages, 200 values were analogously computed on shuffled data. Shuffling was done by randomizing the order of trials and calculating synchronies between events that were not recorded at the same time. The average $W_{k,l}$ was retained as statistically significant if it was greater than the maximum (synchrony) or less than the minimum (desynchrony) of the 200 shuffled values, therefore indicating a two-tailed probability value of $P=0.01$. On a topographical template of the electrode layout, any significant value $W_{k,l}$ was indicated by a line from electrode k to electrode l . Data of all subjects were pooled in the randomization test. In order to estimate the amount of reduction in significant phase-locking values, we have calculated phase synchrony for individual subjects and tested the number of electrode pairs exhibiting significant phase-locking values after initial vs. repeated presentations by means of paired t -tests for each time window.

Data analysis: ERP

In order to investigate the ERP, a 25-Hz low-pass filter was applied to the data before all ERP analyses. Baseline correction was performed by subtracting the mean of the signal during the time window from 400 to 100 ms prior to stimulus onset. Based on previous findings regarding repetition priming (Rugg *et al.*, 1995; Gruber & Müller, 2002), four ERP components were defined on the basis of the grand

mean evoked potential (see Fig. 7): two early components P1 (95–125 ms) and N1 (150–180 ms), and two late components L1 (230–380 ms) and L2 (380–490 ms). Amplitudes were averaged across the defined time windows. Mean amplitudes at electrode sites corresponding to the extended international 10–20 system were analysed using a CONDITION (initial presentations vs. repeated presentations) \times POSITION (three) \times RECORDING SITE (36 electrodes) repeated measurement ANOVA for each of the described components. Post-hoc comparisons were calculated for the three electrode sites showing maximal difference between initial and repeated stimulus presentations by means of paired t -tests.

To depict the topographical distributions of evoked potentials, difference topographies (initial minus repeated presentations) were generated on the basis of all 128 electrode sites separately for each LAG. To allow a direct comparison between topographies of spectral power (gamma band) and ERP amplitude values, data for the ERPs were squared before generating the difference topographies.

Where appropriate, P -values were adjusted by Greenhouse–Geisser correction in all ANOVA models. Means and standard errors are presented.

Time course of the ERP, spectral power and phase synchrony

In order to compare the time course of the ERP, induced and evoked spectral changes, and values of phase synchrony in different frequency bands, the different measures were juxtaposed in Fig. 9. For the ERP, averages across posterior electrode sites for initial and repeated picture presentations (LAG 0 and LAG 1 only) are presented. For induced GBRs the same frequencies as utilized for statistical analysis averaged across posterior electrode sites are depicted for initial and repeated picture presentations. The same frequencies were used for evoked gamma activity. For the representation of evoked and induced alpha activity a frequency band from 8 to 12 Hz is shown. Induced beta activity is presented in a frequency range from 15 to 25 Hz. Furthermore, mean values of phase synchrony between posterior 10–20 electrode sites were represented for the gamma, alpha and beta frequency range for initial and repeated picture presentations. For phase-locking values in the alpha band, a wavelet generated for 10 Hz was used. For the beta band we applied a wavelet generated for 20 Hz. Phase-locking values are given in standard deviations from baseline.

Results

Behavioural data

Subjects detected approximately 99% (SEM = 0.09) of target pictures. Mean RTs to targets (\pm SEM) and detection rates are given in Table 1.

As revealed by a main effect of CONDITION ($F_{1,8} = 101.37$, $P < 0.0001$), subjects reacted significantly faster to repeated as compared with initial target presentations. Furthermore, a significant interaction between CONDITION and POSITION was found ($F_{2,16} = 6.89$, $P < 0.01$). Post-hoc comparisons revealed that immediate picture repetition (LAG 0) resulted in faster RTs as compared with repetitions with LAG 1 ($t_8 = -2.83$, $P < 0.05$) and LAG 4 ($t_8 = -3.58$, $P < 0.001$). Repetitions with LAG 1 and LAG 4 revealed no significant difference. Furthermore, no significant differences between initial target presentations and presentations were found.

Induced and evoked spectral changes

Figure 3 depicts the baseline-corrected TF plots for the average across posterior electrode sites, all experimental conditions and nine subjects. The gamma range and a lower frequency range are shown in separate TF-plots.

TABLE 1. Average reaction times, correct detection rates (\pm SEM) across all nine subjects for initial and repeated picture presentations

	Initial presentations			Repeated presentations		
	A	C	E	B (LAG 0)	D (LAG 1)	F (LAG 4)
Reaction time, RT (ms)	482.2 \pm 16.8	472.5 \pm 14.1	475.8 \pm 12.9	413.1 \pm 18.7	438.7 \pm 13.9	451.2 \pm 13.4
Detection rate (%)	99.3 \pm 0.7	99.4 \pm 0.6	99.5 \pm 0.5	100 \pm 0	99.4 \pm 0.6	99.4 \pm 0.6

Baseline corrected spectral power induced by picture presentations showed a clear peak in a time window from 230 to 300 ms after stimulus onset in a frequency range between 30 and 90 Hz. Alpha power centred around 10 Hz showed a suppression starting about 100 ms after stimulus onset.

Statistical analysis was calculated for a distinct frequency f_0 of each subject's maximal gamma activity within the 30–90 Hz range (Mean \pm SD = 53 \pm 19 Hz). A main effect of CONDITION ($F_{1,8} = 60.86$, $P < 0.0001$) indicated that induced gamma power was significantly higher in the initial as compared with repeated stimulus presentations. No further significant main effect or interaction was found. This shows that there is no significant difference among initial stimulus presentations (Fig. 1A, C and E) and no significant differences between repetitions with three different lags (Fig. 1B, D and F).

Difference topographies between initial and repeated presentations of gamma band power (230–300 ms) are depicted in Fig. 4.

Induced GBR showed a broad posterior distribution with a maximum around electrode site Pz extending mainly to right temporal and frontal areas.

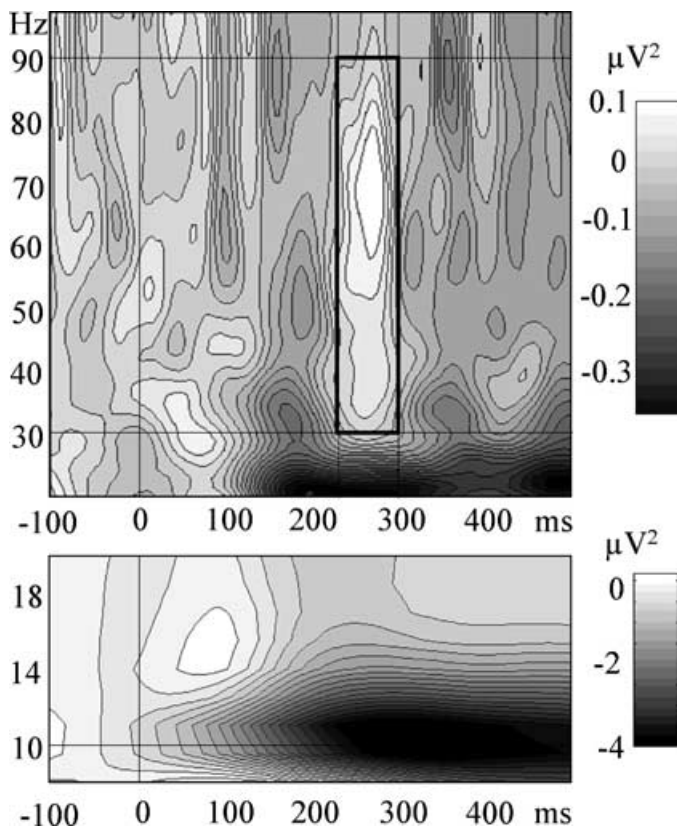


FIG. 3. Time by frequency plot averaged across posterior electrode sites and all experimental conditions for the gamma and lower frequency range. x-axis: time in ms; y-axis: frequency in Hz; grey scale bar: baseline corrected spectral power in μV^2 . Note: the frequency band defined as gamma range and the time window used for further analysis is indicated by a rectangle.

When analysing the time course of spectral gamma power on the basis of the posterior regional mean with maximum amplitude (comprising electrodes P1, P2, CP1, CP2, CPz, P3, P4, PO3, PO4, Pz), we found a significant CONDITION \times TIME interaction ($F_{2,16} = 5.62$, $P < 0.01$) depicted in Fig. 5. The lower part of Fig. 5 depicts induced gamma power separately for each LAG. However, no significant interaction with the factor POSITION was found, indicating no significant differences between LAGs 0, 1 and 4.

As can be seen in Fig. 5, maximal gamma activation was found in the time window from 230 to 300 ms after stimulus onset for initial picture presentations. A comparison of the GBR peak window between initial and repeated presentations revealed a significant reduction ($t_8 = 2.87$, $P < 0.05$). Importantly, post-hoc tests showed that gamma power is different from baseline in all time windows and all conditions (results for bars in upper panel in Fig. 5: $t_8 = 5.68$, $P < 0.001$; $t_8 = 11.47$, $P < 0.0001$; $t_8 = 8.37$, $P < 0.0001$; $t_8 = 5.81$, $P < 0.001$; $t_8 = 4.12$, $P < 0.01$; $t_8 = 4.44$, $P < 0.01$). These effects are not due to baseline differences, as we found no significant differences in the baseline period ($F_{1,8} < 1$).

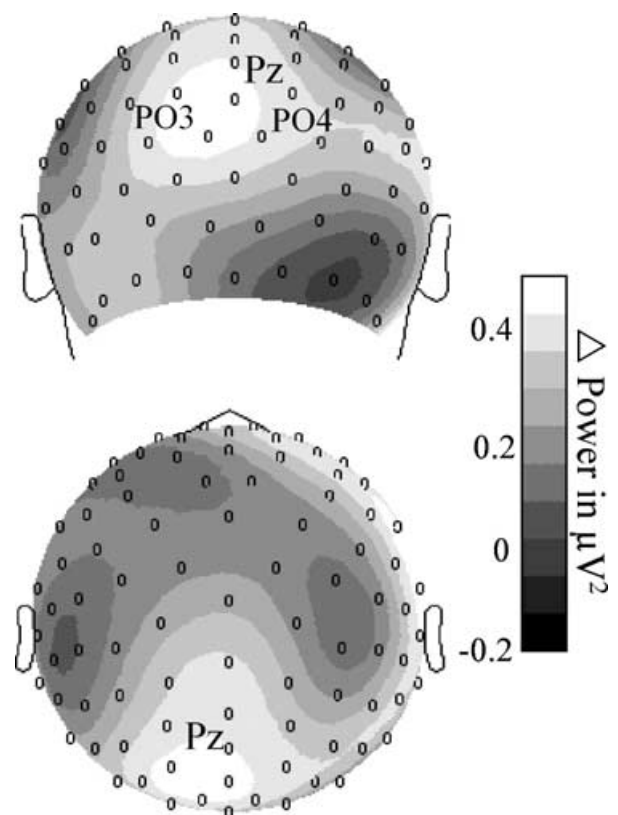


FIG. 4. Grand mean spherical spline difference power-maps (initial minus repeated) based on the individual maximal power in the gamma range in the time window between 230 and 300 ms after stimulus onset.

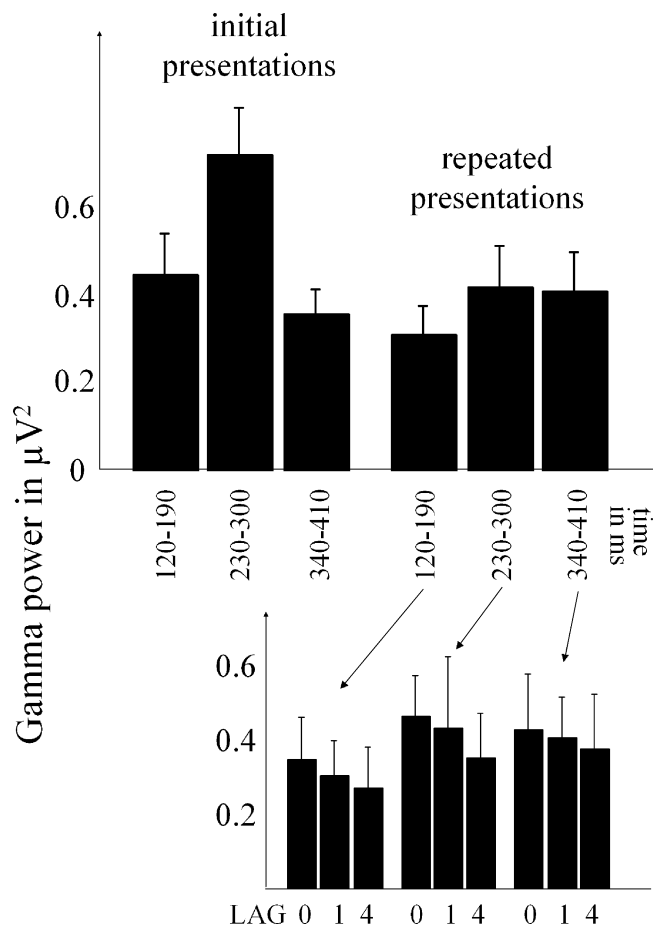


FIG. 5. Upper panel: time course of individual maximal power in the gamma band range (+ SEM) averaged across electrode sites P1, P2, CP1, CP2, CPz, P3, P4, PO3, PO4 and Pz across nine subjects. Lower panel: induced GBR power for each LAG in the three time windows.

With respect to the evoked gamma band response, we found no obvious peak in the TF representations averaged across the six experimental conditions. Thus, we used the same frequencies as for induced GBRs for statistical analysis. This analysis revealed no significant effects.

Further, we found no significant effects for the induced and evoked beta band between 15 and 25 Hz (time window: 100–500 ms), and the induced and evoked alpha band (time window: 100–500 ms).

Phase synchrony

Figure 6 depicts phase synchrony (solid lines) and desynchrony (dashed lines) between extended 10–20 sites for first and repeated stimulus presentations. Besides the above analysed time windows, an additional window from 10 to 80 ms after stimulus was included. For each subject, phase synchrony was computed for his/her distinct maximum frequency f_0 , which was used for the statistical analysis of gamma power. For the initial picture presentations, the most dense pattern of significant phase-locking values was found in the time window of the induced gamma power peak (230–300 ms) predominantly among distant posterior and temporal electrode sites, indicating synchronous neural activity in a broadly distributed network. The number of pairs showing significant phase-locking after initial presentation was significantly higher in the peak time window ($t_8 = 3.45$, $P < 0.01$) and in the time window from 340 to 410 ms ($t_8 = 2.38$, $P < 0.05$), as opposed to repeated pictures.

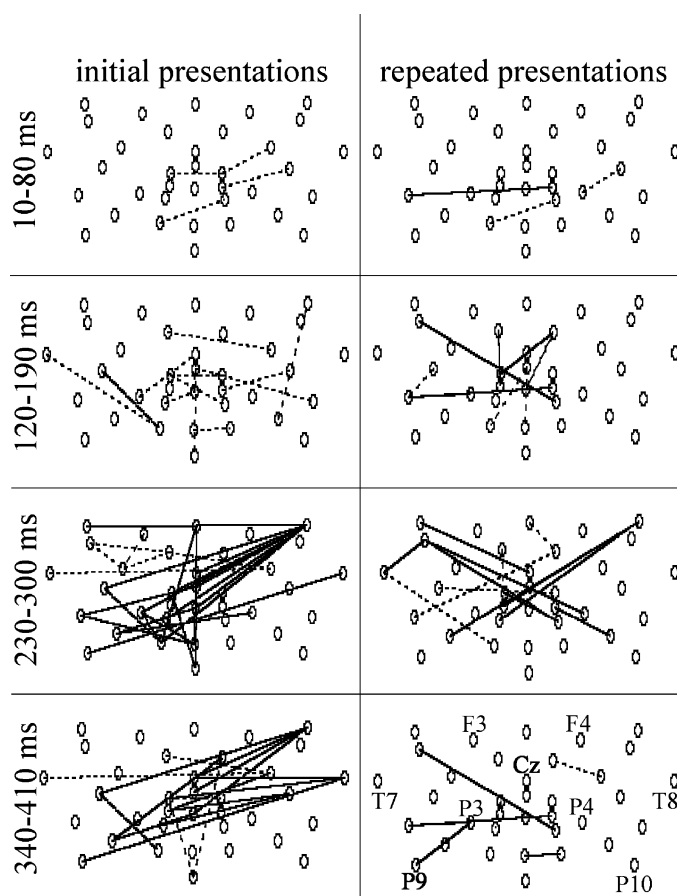


FIG. 6. Synchrony (solid lines) and desynchrony (dashed lines) between 10 and 20 electrode pairs for initial and repeated picture presentations. Lines are drawn only if the phase-locking value is beyond the distribution of shuffled data ($P < 0.01$).

Visual ERP

Figure 7A depicts the ERPs at 10–20 electrode sites averaged across initial presentations (bold black line) and separately for repetitions with LAG 0 (thin black line), LAG 1 (thin grey line) and LAG 4 (bold grey line). Furthermore, in Fig. 7B the ERP averaged across electrode sites O1, PO7, P3 and O2, PO8, P4 is depicted.

We found no significant differences for the P1 and N1 components between the experimental conditions. The late component L1 (230–380 ms) revealed a significant $\text{CONDITION} \times \text{POSITION} \times \text{ELECTRODE}$ interaction ($F_{70,560} = 2.15$, $P < 0.05$), reflecting a reduction in positivity for repeated pictures at posterior electrode sites. This effect was found to be reversed at anterior sites. Furthermore, the reduction in amplitude dissolved for repeated presentations with LAG 4. Difference topographies (initial minus repeated presentations) for each LAG on the basis of squared amplitudes are depicted in Fig. 8. These voltage difference maps revealed two distinct posterior peaks for repetitions with LAG 0 and LAG 1, but not for LAG 4.

Post-hoc tests for the three electrode sites, which showed a maximal difference between initial and repeated presentations (P3, O1 and Fz; see Fig. 7) resulted in a significant decrease in amplitude for LAG 0 and LAG 1 (P3: initial vs. repeated-LAG 0: $t_8 = 2.61$, $P < 0.05$; P3: initial vs. repeated-LAG 1: $t_8 = 2.55$, $P < 0.05$; O1: initial vs. repeated-LAG 0: $t_8 = 3.26$, $P = 0.01$; O1: initial vs. repeated-LAG 1: $t_8 = 2.59$, $P < 0.05$; Fz: initial vs. repeated-LAG 0: $t_8 = -2.31$, $P = 0.05$; Fz: initial vs. repeated-LAG 1: $t_8 = -2.51$, $P < 0.05$). No significant differences were found for LAG 4.

The late component L2 (380–490 ms) resulted in a significant $\text{CONDITION} \times \text{POSITION} \times \text{ELECTRODE}$ interaction ($F_{70,560} = 2.52, P < 0.01$), reflecting a decrease in peak-to-peak negativity from L1 to L2 for repeated pictures at parietal electrode sites. Post-hoc tests for three electrode sites showing a maximal difference between initial and repeated presentations (see Fig. 7) showed significant effects for electrode sites CP1, CP2 and CPz. (CP1: initial vs. repeated-LAG 4: $t_8 = -3.22, P = 0.01$; CP2: initial vs. repeated-LAG 4: $t_8 = -4.38, P < 0.01$; CPz: initial vs. repeated-LAG 4:

$t_8 = -4.83, P = 0.001$). No significant differences were found for LAG 0 and LAG 1.

Time course of the ERP, spectral power and phase synchrony

Figure 9 depicts the ERP, induced and evoked spectral changes, and phase-locking values in different frequency bands (significant differences are indicated by stippled areas). Here a number of interesting patterns can be observed. The ERPs averaged across posterior electrode sites for initial and repeated picture presentations depict the

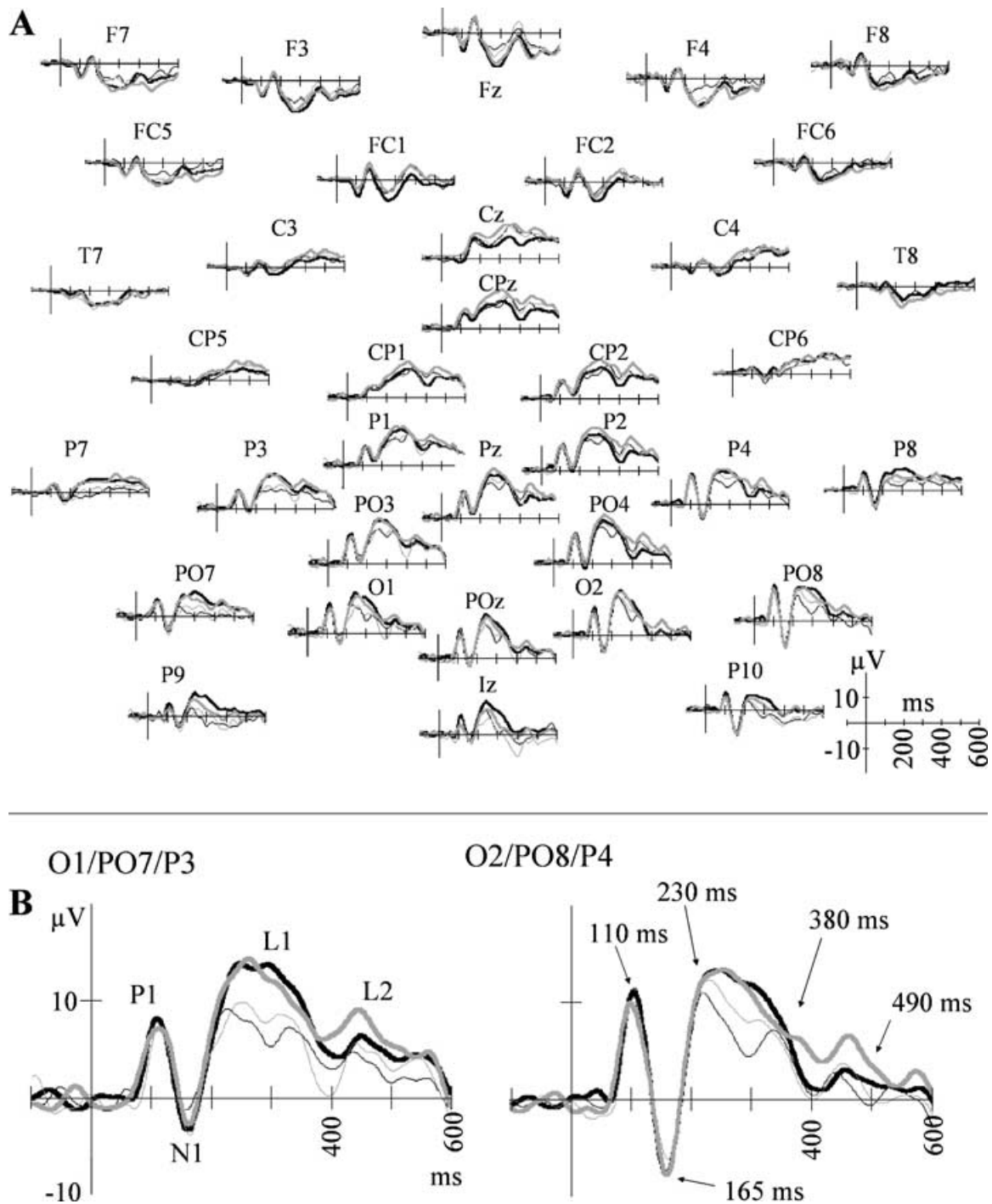


FIG. 7. (A) Grand mean baseline corrected ERPs averaged across initial presentations (bold black line) and separately for repetitions with LAG 0 (thin black line), LAG 1 (thin grey line) and LAG 4 (bold grey line) at 10–20 electrode sites. (B) Grand mean baseline corrected ERP averaged across electrode sites O1, PO7, P3 (left) and O2, PO8, P4 (right).

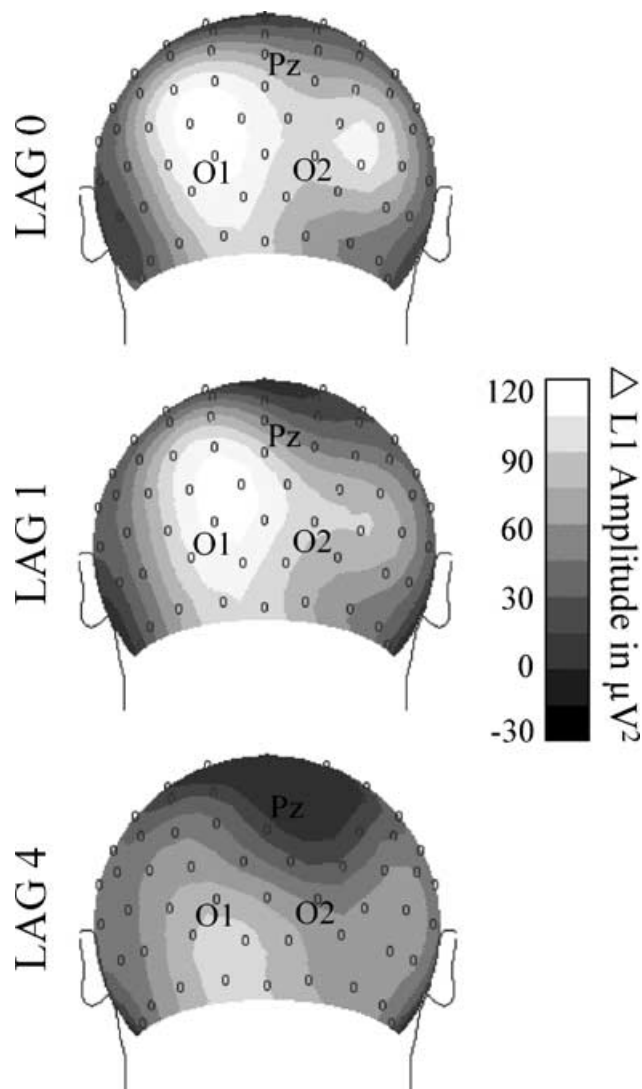


FIG. 8. Grand mean spherical spline difference power-maps (initial minus repeated) for each LAG based on the squared amplitude of the L1 component of the ERP (230–380 ms post-stimulus).

suppression effect as described above (due to the fact repetition effects decayed at LAG 4, an average across LAG 0 and LAG 1 repetitions is presented). The L1 component peaked at about 300 ms after stimulus onset. Interestingly, the peak of the L2 component matches approximately the averaged RTs for target stimuli.

Induced gamma power peaks at 260 ms after stimulus onset. Given a mean wavelet duration in the 30–90 Hz band of approximately 40 ms, the gamma peak covers a time window from 220 to 300 ms in the time domain. Therefore, the peak of gamma power and the L1 amplitude are similar in the time domain. No equivalent to the L2 component can be observed in the gamma range. Phase-locking values in the gamma range averaged across posterior electrode sites revealed a maximum in the same time window as the induced gamma power peak.

In the alpha frequency range, none of the measures revealed a difference between experimental conditions. Evoked alpha power peaks at about 150 ms after stimulus onset. This latency range matches the P1/N1 complex in the ERP. Induced alpha power showed a decrease from about 100 ms after stimulus onset as compared with baseline. Interestingly, alpha synchrony showed an increase from

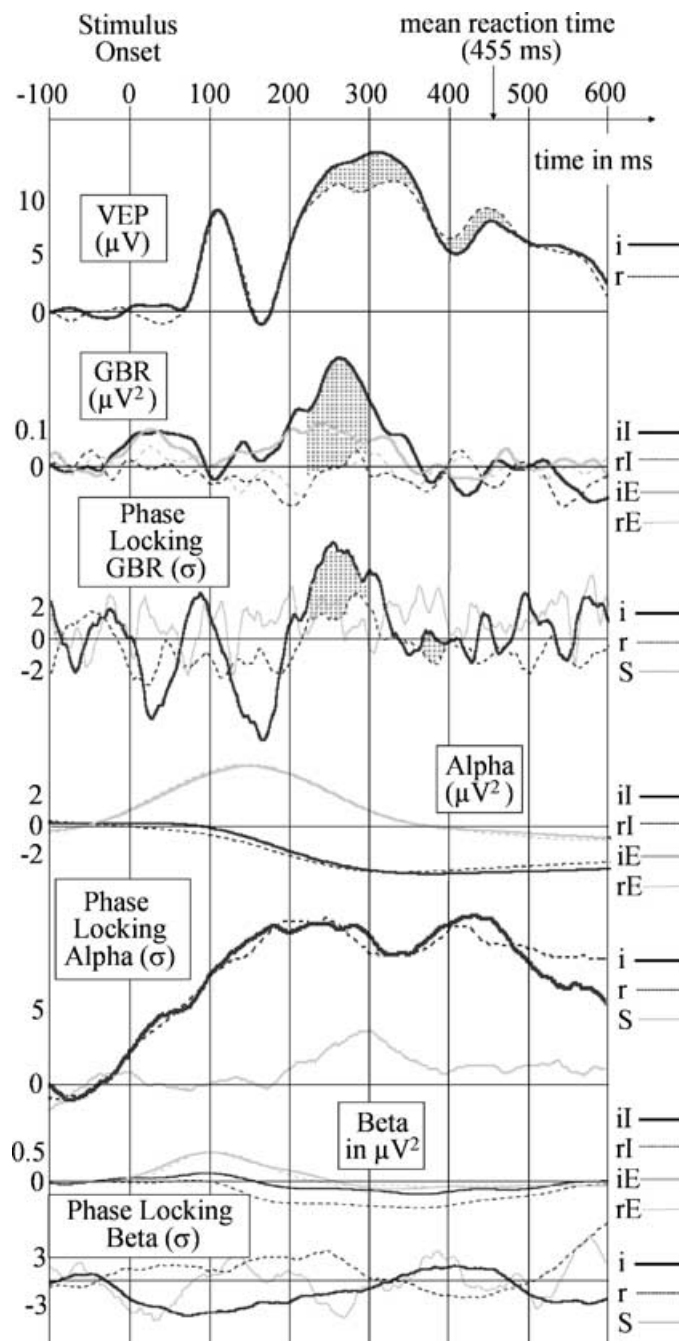


FIG. 9. Grand mean ERP, induced and evoked spectral power changes in the gamma, alpha and beta frequency range, and phase locking values. Initial and repeated presentations averaged across posterior 10–20 electrode sites are presented. In the ERP, repetitions with LAG 0 and LAG 1 are averaged. Significant differences are indicated by stippled areas. Abbreviations: E, evoked spectral power; GBR, gamma band response; i, initial presentations; I, induced spectral power; r, repeated presentations; S, shuffled data; VEP, visual evoked potential.

stimulus onset until reaching a plateau at approximately 200 ms, indicating that synchronization co-existed with periods of below-baseline alpha power. Values of alpha synchrony decreased in the time range of the L2 ERP component and the time range of mean RTs to target stimuli.

None of the measurements in the beta frequency range showed any significant differences.

Discussion

The present study was designed to provide evidence that the reduction of induced GBRs and phase synchrony during repeated picture presentations is a robust and replicable neuronal correlate of repetition priming. Furthermore, we intended to exclude habituation as an alternative explanation for previously reported suppression effects in the gamma band during picture repetition (Gruber & Müller, 2002).

Behavioural data verified that our experimental set-up was suitable to fulfil the criteria of repetition priming. Subjects showed speeded RTs for repeated as compared with initial picture presentations, indicating a more efficient processing of primed objects.

After the first presentation of an object, induced GBRs showed a broad posterior scalp distribution. Importantly, the augmentation of spectral power was accompanied by a dense pattern of significant phase-locking values between distant electrode sites. Whereas an increase of spectral power alone might be an insufficient marker of a synchronized cell assembly (Lachaux *et al.*, 1999), the combined information points towards integrative cortical activity in the larger scale (Varela *et al.*, 2001). This assumption is in line with previous studies, which have shown that if no unequivocal object representation can be established, neither power nor phase synchrony exhibited such a strong increase as in conditions in which object representations can easily be established (for recent examples, see Rodriguez *et al.*, 1999; Gruber *et al.*, 2002).

Regarding repeated object presentations, we replicated our previous findings (Gruber & Müller, 2002). Again we found a decrease in induced gamma power and a marked reduction in electrode pairs exhibiting significant phase-locking values after the second presentation of the same object. Based on the assumption that a neuronal assembly, which codes features of an object becomes sparser and more selective with repeated stimulus experience (Desimone, 1996; Wiggs & Martin, 1998), we interpret our findings as a physiological correlate of such a 'sharpening' mechanism. Due to spatial summation in macroscopic EEG recordings, activity within a sparser network must result in a decrease of induced gamma band amplitude and a reduced number of electrode pairs exhibiting significant phase-locking. Importantly, gamma power after repeated stimulus presentation is still well above baseline level, with a number of electrode pairs still showing significant phase-locking. We see this pattern as supportive for the above hypothesis.

A possible alternative reason for the decrease in gamma activity might be the habituation of responses with picture repetitions. We are confident to rule out that alternative explanation, as the present experiment was especially designed to control for habituation by intervening a number of different stimuli between first and repeated stimuli. If our results would be a mere effect of habituation, one would expect no modulation of oscillatory activity at repetitions with LAG 1 and LAG 4.

From the scalp topography of induced GBRs and the pattern of phase synchrony, it seems very likely – and parallels previous work (Keil *et al.*, 1999; Gruber *et al.*, 2001, 2002) – that the integration of activity across multiple visual areas has contributed to these findings. Although the idea of a synchronized network involving widespread cortical areas fits well with our current hypothesis, it has to be mentioned that this interpretation is speculative at the moment, because scalp recordings do not allow us to draw direct conclusions on underlying cortical generators. However, the reduction in gamma activity to repeated stimuli at parietal electrode locations appears to be consistent with imaging studies of priming showing a parietally focused reduction in blood flow-dependent measures of neural activity to repeated stimuli (Buckner *et al.*, 1996; Schacter & Buckner, 1998; Henson *et al.*, 2000; Henson & Rugg, 2003).

Oscillatory brain activity was not only reported in the induced, but also in the evoked gamma range (Herrmann *et al.*, 1999), and in lower frequency bands (Klimesch, 1995, 1997; Sarnthein *et al.*, 1998; von Stein *et al.*, 2000). We therefore extended our analysis to evoked oscillatory activity and frequency bands lower than 20 Hz. However, we found no significant effects in these measures, pointing towards a functionally specific role of induced GBRs in perceptual priming as compared with other oscillatory phenomena.

In the ERP, results for LAG 0 and LAG 1 showed a decreased positivity to repeated stimuli. This is in line with previous studies using visual stimuli (Rugg *et al.*, 1995; Van Petten & Senkfor, 1996; Penney *et al.*, 2001; Gruber & Müller, 2002). Interestingly, whereas the suppression in the gamma band was not modulated by the lag of the repetition, the effects in the ERP decayed at repetitions with LAG 4. This replicates previous findings (Nagy & Rugg, 1989; Rugg *et al.*, 1997), which also showed that the ERP suppression effect does not survive more than a few items. Furthermore, effects in the ERP showed a topographically more distinct distribution around electrode sites P3 and P4 as compared with the broad distribution of the effect in the gamma band. Although we cannot totally rule out that a certain degree of blurring is based on the lower signal-to-noise ratio of GBRs as opposed to the ERP, in a series of studies it has been shown that high-frequency brain activity is highly sensitive to different associative contents of a stimulus, different tasks and different sensory modalities (for recent reviews see: Tallon-Baudry & Bertrand, 1999; Keil *et al.*, 2001). This provides empirical evidence that broader GBR scalp distributions are not a consequence of lower signal-to-noise ratios. Thus, the present results provide further evidence that ERPs play a functionally complementary role in perception as compared with induced GBRs. Whereas induced GBRs might be a signature of a cortical object representation over widespread cortical areas, the visual evoked response may reflect differences in the activity of more distinct and more transient repetition-sensitive brain structures (Rugg *et al.*, 1995). The question if the reduction of amplitude in the evoked response is due to a 'sharpening' process on a different level of processing must be examined in future studies.

A possible alternative explanation for the present findings is that initial as compared with repeated picture presentations were attracting more attention. Indeed, induced GBRs are known to be modulated by attention (Gruber *et al.*, 1999; Müller & Gruber, 2001; Müller *et al.*, 2000). In order to control for attention effects, we introduced a target detection task in which the occurrence of a target was unpredictable and, thus, subjects had to pay the same amount of attention to every picture presentation. Based on the average target detection rate of 99%, it is very unlikely that attentional effort is reduced after the first presentation.

A possible concern regarding the analysis of phase synchrony is that the signal's gamma amplitude induced by repeated pictures was too small to establish a well-defined phase signal and draw robust conclusion on phase-locking values. However, spectral power values, which were significantly higher than baseline for initial and repeated presentations, seem to exclude this possibility. We can also exclude that our results were confounded by muscle activity, as one might expect a maximum of activity at electrode sites close to the neck muscles, which was not the case in our study. Regarding the discussion of possible influences of volume conduction on the calculation of phase-locking, we refer to Lachaux *et al.* (1999) and Gruber & Müller (2002).

In summary, the present experiment has several implications for the understanding of neural mechanism underlying repetition priming. The presentation of a primed object leads to repetition suppression within a network, which integrates neural activity from different cortical areas. This suppression might be linked to a sharpening of

the cortical object representation. This suppression effect should be kept in mind for designing future studies, which focus on the measurement of high-frequency brain activity. In particular, the repetition of stimulus material should be avoided, if this is not an important aspect of the to-be-tested hypothesis.

While we are aware of the fact that the quite simplistic 'sharpening' metaphor has to be treated with some caution, we believe that it seems to be a useful working hypothesis for future studies regarding oscillatory brain activity related to priming processes. Because research in the field of oscillatory dynamics in the human brain is still at its very beginning, further studies have to answer the question if this 'sharpening' is due to the fact that parts of an associative network drop out completely, or if the anatomical extent of the networks stays the same and only the number of neurons in the areas comprising the network is reduced.

Acknowledgement

Research was supported by grants from the Deutsche Forschungsgemeinschaft.

Abbreviations

GBR, gamma band response; EEG, electroencephalogram; ERP, event-related potential; RT, reaction time; TF, time by frequency.

References

- Bertrand, O. & Pantev, C. (1994) Stimulus frequency dependence of the transient oscillatory auditory evoked response (40 Hz) studied by electric & magnetic recordings in human. In Pantev, C., Elbert, T. & Lütkenhöner, B. (Eds), *Oscillatory Event-Related Brain Dynamics*. Plenum Press, New York, USA, pp. 231–242.
- Brown, M.W. & Aggleton, J.P. (2001) Recognition memory: what are the roles of the perirhinal cortex and hippocampus? *Nat. Rev. Neurosci.*, **2**, 51–61.
- Buckner, R.L., Raichle, M.E., Miezin, F.M. & Petersen, S.E. (1996) Functional anatomic studies of memory retrieval for auditory words and visual pictures. *J. Neurosci.*, **16**, 6219–6235.
- Desimone, R. (1996) Neural mechanisms for visual memory and their role in attention. *Proc. Natl Acad. Sci. USA*, **93**, 13494–13499.
- Gruber, T., Keil, A. & Müller, M.M. (2001) Modulation of induced gamma band responses and phase synchrony in a paired associate learning task in the human EEG. *Neurosci. Lett.*, **316**, 29–32.
- Gruber, T., Keil, A. & Müller, M.M. (2002) Modulation of induced gamma band responses in a perceptual learning task in human EEG. *J. Cog. Neurosci.*, **14**, 732–744.
- Gruber, T. & Müller, M.M. (2002) Effects of picture repetition on induced gamma band responses, evoked potentials, and phase synchrony in the human EEG. *Brain Res. Cogn Brain Res.*, **13**, 377–392.
- Gruber, T., Müller, M.M., Keil, A. & Elbert, T. (1999) Selective visual-spatial attention alters induced gamma band responses in the human EEG. *Clin. Neurophysiol.*, **110**, 2074–2085.
- Henson, R.N. & Rugg, M.D. (2003) Neural response suppression, haemodynamic repetition effects, and behavioural priming. *Neuropsychologia*, **41**, 263–270.
- Henson, R., Shallice, T. & Dolan, R. (2000) Neuroimaging evidence for dissociable forms of repetition priming. *Science*, **287**, 1269–1272.
- Herrmann, S., Mecklinger, A. & Pfeifer, E. (1999) Gamma responses and ERPs in a visual classification task. *Clin. Neurophysiol.*, **110**, 636–642.
- Junghöfer, M., Elbert, T., Leiderer, P., Berg, P. & Rockstroh, B. (1997) Mapping EEG-potentials on the surface of the brain: a strategy for uncovering cortical sources. *Brain Topogr.*, **9**, 203–217.
- Junghöfer, M., Elbert, T., Tucker, D. & Braun, C. (1999) The polar effect of average reference: a bias in estimating the head surface integral in EEG recording. *Clin. Neurophysiol.*, **110**, 1149–1155.
- Junghöfer, M., Elbert, T., Tucker, D.M. & Rockstroh, B. (2000) Statistical control of artifacts in dense array EEG/MEG studies. *Psychophysiology*, **37**, 523–532.
- Keil, A., Gruber, T. & Müller, M.M. (2001) Functional correlates of macroscopic high-frequency brain activity in the human visual system. *Neurosci. Biobehav. Rev.*, **25**, 527–534.
- Keil, A., Müller, M.M., Ray, W.J., Gruber, T. & Elbert, T. (1999) Human gamma band activity and perception of a gestalt. *J. Neurosci.*, **19**, (electronic publication).
- Klimesch, W. (1995) Memory processes described as brain oscillations. *Psychology*, **6**, 1–15.
- Klimesch, W. (1997) EEG-alpha rhythms and memory processes. *Int. J. Psychophysiol.*, **26**, 319–340.
- Lachaux, J.P., Rodriguez, E., Martinerie, J. & Varela, F.J. (1999) Measuring phase synchrony in brain signals. *Hum. Brain Mapp.*, **8**, 194–208.
- Malsburg, C.v.d. & Schneider, W. (1986) A neural cocktail-party processor. *Biol. Cybern.*, **54**, 29–40.
- Milner, P.M. (1974) A model for visual shape recognition. *Psychol. Rev.*, **81**, 521–535.
- Miltner, W.H.R., Braun, C., Arnold, M., Witte, H. & Taub, E. (1999) Coherence of gamma-band activity as a basis for associative learning. *Nature*, **397**, 434–436.
- Müller, M.M., Bosch, J., Elbert, T., Kreiter, A., Valdes Sosa, M., Valdes Sosa, P. & Rockstroh, B. (1996) Visually induced gamma-band responses in human electroencephalographic activity – a link to animal studies. *Exp. Brain Res.*, **112**, 96–102.
- Müller, M.M. & Gruber, T. (2001) Induced gamma-band responses in the human EEG are related to attentional information processing. *Vis. Cog.*, **8**, 579–592.
- Müller, M.M., Gruber, T. & Keil, A. (2000) Modulation of induced gamma band activity in the human EEG by attention and visual information processing. *Int. J. Psychophysiol.*, **38**, 283–299.
- Nagy, M.E. & Rugg, M.D. (1989) Modulation of event-related potentials by word repetition: the effects of inter-item lag. *Psychophysiology*, **26**, 431–436.
- Penney, T.B., Mecklinger, A. & Nessler, D. (2001) Repetition related ERP effects in a visual object target detection task. *Brain Res. Cogn Brain Res.*, **10**, 239–250.
- Priestley, M.B. (1988) *Non-Linear and Non-Stationary Time Series Analysis*. Academic Press, London.
- Pulvermüller, F. (1996) Hebb's concept of cell assemblies and the psychophysiology of word processing. *Psychophysiology*, **33**, 317–333.
- Rodriguez, E., George, N., Lachaux, J.P., Martinerie, J., Renault, B. & Varela, F.J. (1999) Perception's shadow: long-distance synchronization of human brain activity. *Nature*, **397**, 430–433.
- Rugg, M.D., Mark, R.E., Gilchrist, J. & Roberts, R.C. (1997) ERP repetition effects in indirect and direct tasks: effects of age and interitem lag. *Psychophysiology*, **34**, 572–586.
- Rugg, M.D., Soardi, M. & Doyle, M.C. (1995) Modulation of event-related potentials by the repetition of drawings of novel objects. *Brain Res. Cogn Brain Res.*, **3**, 17–24.
- Sarnthein, J., Petsche, H., Rappelsberger, P., Shaw, G.L. & von Stein, A. (1998) Synchronization between prefrontal and posterior association cortex during human working memory. *Proc. Natl Acad. Sci. USA*, **95**, 7092–7096.
- Schacter, D.L. & Buckner, R.L. (1998) Priming and the brain. *Neuron*, **20**, 185–195.
- Singer, W. & Gray, C.M. (1995) Visual feature integration and the temporal correlation hypothesis. *Annu. Rev. Neurosci.*, **18**, 555–586.
- Snodgrass, J.G. & Vanderwart, M. (1980) A standardized set of 260 pictures: norms for name agreement, image agreement, familiarity and visual complexity. *J. Exp. Psychol. [Hum. Learn.]*, **6**, 174–215.
- von Stein, A., Chiang, C. & Konig, P. (2000) Top-down processing mediated by interareal synchronization. *Proc. Natl Acad. Sci. USA*, **97**, 14748–14753.
- Tallon-Baudry, C. & Bertrand, O. (1999) Oscillatory gamma activity in humans and its role in object representation. *Trends Cogn. Sci.*, **3**, 151–162.
- Tallon-Baudry, C., Bertrand, O., Delpuech, C. & Pernier, J. (1997) Oscillatory gamma-band (30–70 Hz) activity induced by a visual search task in human. *J. Neurosci.*, **17**, 722–734.
- Tallon-Baudry, C., Bertrand, O. & Fischer, C. (2001) Oscillatory synchrony between human extrastriate areas during visual short-term memory maintenance. *J. Neurosci.*, **21**, RC177.
- Tallon-Baudry, C., Bertrand, O., Peronnet, F. & Pernier, J. (1998) Induced gamma-band activity during the delay of a visual short-term memory task in humans. *J. Neurosci.*, **18**, 4244–4254.
- Tulving, E. & Schacter, D.L. (1990) Priming and human memory systems. *Science*, **247**, 301–306.
- Van Petten, C. & Senkfor, A.J. (1996) Memory for words and novel visual patterns: repetition, recognition, and encoding effects in the event-related brain potential. *Psychophysiology*, **33**, 491–506.
- Varela, F., Lachaux, J.P., Rodriguez, E. & Martinerie, J. (2001) The brainweb: phase synchronization and large-scale integration. *Nat. Rev. Neurosci.*, **2**, 229–239.
- Wiggs, C.L. & Martin, A. (1998) Properties and mechanisms of perceptual priming. *Curr. Opin. Neurobiol.*, **8**, 227–233.

Copyright of European Journal of Neuroscience is the property of Blackwell Publishing Limited and its content may not be copied or emailed to multiple sites or posted to a listserv without the copyright holder's express written permission. However, users may print, download, or email articles for individual use.